RSPO2-based peptibodies conjugated with pyrrolobenzodiazepine dimer or camptothecin analogs demonstrate potent anti-tumor activity by targeting the three receptors LGR4/5/6

Yukimatsu Toh[1], Jianghua Tu[1], Ling Wu[1], Adela Aldana[1], Jake Wen[1], Xiaowen Liang[2], Li Li[1], Sheng Pan[1], Jie Cui[2], and Qingyun J. Liu[1]*

From: [1]The Brown Foundation Institute of Molecular Medicine, Center for Translational Cancer Research, University of Texas Health Science Center at Houston, Houston, TX 77030 USA; [2]Wntrix, K2Bio, 2710 Reed Rd., Suite 160, Houston, TX 77051.

*To whom correspondence should be addressed to: Qingyun J. Liu, Brown Foundation Institute of Molecular Medicine, University of Texas Health Science Center at Houston, 1825 Pressler St., Suite 330E, Houston, TX 77030, email: Qingyun.liu@uth.tmc.edu; ORCID: 0000-0001-7683-5088.

Abstract

LGR4/5/6 (leucine-rich repeat containing, G protein-coupled receptors 4, 5, and 6) are three homologous receptors that are co-expressed or alternately expressed at high levels in tumor cells of colorectal cancer and high-risk neuroblastoma. Simultaneous targeting of all three receptors may provide increased efficacy or overcome drug resistance due to tumor heterogeneity and cancer cell plasticity. LGR4/5/6 all bind to R-spondins (RSPOs) with high affinity and potentiate Wnt/β-catenin signaling in response. Previously, we showed that a peptibody based on a mutant RSPO4 furin domain that bound to LGR4/5/6 without potentiating Wnt/β-catenin signaling was able to deliver cytotoxins into cancer cells that express any of the three receptors. We have now generated a mutant RSPO2 furin domain that retains high affinity binding to LGR4/5/6 without signaling activity. Peptibodies based on this RSPO2 furin mutant were conjugated with either pyrrolobenzodiazepine dimer or camptothecin derivative, and the resulting peptibodydrug conjugates (PDCs) showed potent and specific cytotoxic activity in neuroblastoma and colorectal cancer cell lines expressing any of LGR4/5/6 in vitro and robust anti-tumor activity in vivo. The results support the potential of RSPO2-based PDCs for the treatment of colorectal cancer, high-risk neuroblastoma, and other cancers that express LGR4/5/6.

Keywords: Neuroblastoma, colorectal cancer, RSPO2, peptibody, peptibody-drug conjugate, pyrrolobenzodiazepine dimer, camptothecin

1. Introduction

LGR4/5/6 (leucine-rich repeat containing, G protein-coupled receptor 4, 5, and 6) are three related membrane receptors with a large extracellular domain (ECD) and a seven transmembrane (7TM) domain typical of the rhodopsin family of G protein-coupled receptors[1-3]. LGR4 is broadly expressed in epithelial tissues with critical roles in cell proliferation and migration during organ development whereas LGR5 is expressed mostly in adult stem cells in the gastrointestinal (GI) tract and some other tissues [2, 4, 5]. R-spondins are a group of four related secreted proteins (RSPO1/2/3/4) that play essential roles in normal development and survival of adult stem cells[6]. RSPOs function as ligands of LGR4/5/6 to potentiate Wnt signaling and support stem cell growth[7-10]. Mechanistically, RSPO-LGR4 form a complex to inhibit the function of RNF43 and ZNRF3, two E3 ligases that ubiquitinate Wnt receptors for degradation, leading to higher Wnt receptor levels and stronger signaling[11-14]. In contrast, LGR5 does not potentiate Wnt signaling through sequestering of the E3 ligases [13].

LGR4/5/6 are often co-expressed or alternately expressed in various cancer types, particularly in cancers of the gastrointestinal system, with LGR4 co-expressed with LGR5 or LGR6.[15-20] Furthermore, LGR5 has been shown to be enriched in cancer stem cells of colorectal cancer (CRC) [21-24] and LGR5-positive cancer cells were shown to fuel the growth of primary tumors and metastasis [25, 26]. LGR6 is a marker of cancer stem cells of squamous cell carcinoma [24]. The Cancer Genome Atlas's (TCGA's) RNA-Seq data of colorectum, liver, and stomach cancers confirmed that LGR4 expression at high levels in nearly all cases while LGR5 and LGR6 were co-expressed with LGR4 in the majority of CRC and substantial fractions of liver and stomach cancer. LGR4/5/6 were also found to be highly expressed in liver metastasis of CRC[27, 28]. On the other hand, LGR5 was also found to be one of the genes that were most enriched in neuroblastoma (NB) cells selected for sphere-forming and metastasis capability[29]. Subsequent studies reported that LGR5 expression is associated with aggressive diseases in NBs with or without *MYCN* amplification[30-33] LGR5 expression was also found to be highly enriched in end-stage tumors in the mouse model of NB driven by *MYCN* overexpression[34]. Knockdown of LGR5 in LGR5-high NB cell lines led to reduced MAPK signaling and decreased cell growth[31]. Recently, LGR5 expression was found to be increased in drug-resistant NB cell lines[35]. Furthermore, analysis of TCGA's neuroblastoma RNA-Seq data revealed that LGR4 was also expressed in the majority of NB tumors. Overall, these expression data support that simultaneous targeting of LGR4/5/6 may provide an effective approach for the treatment of metastatic CRC and high-risk neuroblastoma.

Antibody-drug conjugates (ADCs) have become a major modality of cancer therapy [36, 37]. ADCs consist of a monoclonal antibody linked to a cytotoxic payload via a chemical linker [36, 37]. The antibody component specifically targets antigens overexpressed on cancer cells, delivering potent cytotoxic agent directly to the tumor, thereby reducing systemic toxicity. Previously, we reported that anti-LGR5 ADC conjugated with pyrrolobenzodiazepine dimer (PBD) had robust anti-tumor activity in neuroblastoma tumor models[33]. We also reported that a modified, antagonistic RSPO4 peptibody that was based on the fusion of a modified RSPO4 furin domain with human IgG1-Fc to deliver the cytotoxin monomethyl auristatin E (MMAE) or a camptothecin analog (CPT2) into cancer cells expressing any LGR4/5/6[38, 39], which is similar to the ADC approach except that the ligand-drug conjugate enables the targeting of LGR4/5/6 simultaneously. Here we report the generation and characterization of RSPO2-based peptibody-drug conjugate (PDC) using PBD and CPT2 in preclinical models of CRC and NB. The PBD- and CPT2-based RSPO2 PDCs showed highly potent cytotoxic activity across CRC and NB cell lines expressing LGR4/5/6 at various levels in vitro and robust anti-tumor effect in cell line xenograft models in vivo.

2. Materials and Methods

2.1. Cell lines

The neuroblastoma and CRC cell lines SK-N-AS, SK-N-BE, CHP212, HT29, SW620, and RKO were purchased from the American Type Culture Collection (ATCC). CRISPR/Cas9-mediated gene editing via lentiviral vectors, as described previously[40, 41], was utilized to generate LGR5-knockout variants of the SK-N-AS, SK-N-BE, and CHP212 cell lines. HEK292T cells stably expressing human LGR4, LGR5, or LGR6 and SuperTopFlash (STF) cell line were described before[7]

2.2. PDC preparation and characterization

The sequences encoding wild-type RSPO2 furin domain (R203) fused to human IgG1-Fc were described previously[41]. Its mutants (R291, R299, R290, and R296) were generated and cloned into the mammalian protein expression vector pCEP5 using the In-Fusion cloning method. To enable microbial transglutaminase (MTGase)-mediated site-specific conjugation, mutations were introduced at the N297 glycosylation site, generating N297A Fc variants for R291 and R299, and N297Q Fc variants for R290 and R296. Protein production and characterization were carried out as described before[41]. Briefly, peptibodies were expressed in Expi293™ cells (Thermo Fisher Scientific) by transient transfection, purified by CaptivA® HF Protein A Resin (Repligen) via gravity

flow, and further refined through size-exclusion chromatography on a HiLoad 16/600 Superdex 200 pg column (Cytiva).

Subsequently, purified peptibodies (5 mg/mL in PBS, pH 7.2) were conjugated overnight at room temperature using 8% Activa® TI Transglutaminase (Ajinomoto) and 40 molar equivalents of amino-PEG4-azide linker (BroadPharm) or N-(Amino-PEG2)-N-bis(PEG3-Azide) linker (BroadPharm). Unreacted linker and residual MTGase were removed through Protein A resin treatment with gentle mixing at room temperature for 2 hours. The resulting conjugate was then reacted with 1.5 molar equivalents of linker-drug at room temperature for an additional 4 hours, provided as a 20 mg/m in dimethyl sulfoxide (DMSO) stock solution of either DBCO-PEG8-VA-PAB-SG3199 or DBCO-PEG8-Val-Lys-Gly-14-aminomethyl (CPT2) (Levena Biopharma), ensuring the final DMSO concentration remained below 10% (v/v). Following the reaction, excess reagents were removed by size-exclusion chromatography, and the final peptibody-drug conjugate (PDC) was buffer-exchanged into formulation buffer (20 mM sodium succinate, 6% trehalose, pH 5.0) stored at -80 °C until further use.

The PDC samples were analyzed using an Agilent 6538 Q-TOF LC/MS coupled to an Agilent 1200 HPLC as described before [33]. Separation occurred on an Agilent PLRP-S reversed-phase column using a gradient of acetonitrile-water-formic acid solvents. Mass spectrometry was performed in positive ESI mode, and raw data were processed using Agilent MassHunter BioConfirm software for molecular mass determination.

2.3. Cell based signaling and binding assay

Potentiation of Wnt/β-catenin signaling assay was performed using the SuperTopFlash cell line and 10% conditioned Wnt3A media as described before[7]. Whole-cell binding assays were conducted as previously described[7]. In brief, stable HEK293-LGR4, HEK293-LGR5-DeltaC, and HEK293-LGR6 cells were seeded onto poly-D-lysine–coated black, clear-bottom 96-well plates and cultured overnight. Fc-tagged peptibodies and PDCs were serially diluted and added to the cells, followed by incubation on ice for 1 hour. Cells were then washed and fixed with 4.2% paraformaldehyde and incubated with anti-human Alexa Fluor 555 antibody. Fluorescence emission at 550 nm was measured using a plate reader (Tecan), and dose-response curves were fitted using GraphPad Prism (Boston MA) to calculate the half-maximum binding constant (KD). All assays were performed at least three times, with duplicates or triplicates per experiment.

2.4. Cytotoxic assay

For cytotoxicity assays, cells were seeded at a density of 3×10^3 cells per well in 96-well plates (Costar Assay Plate, Corning). Serial dilutions of PDCs as indicated were then added. After incubation for 5 days, cell viability was assessed using the CellTiter-Glo® Luminescent Cell Viability Assay (Promega, Madison, WI) and measured on a TECAN Infinite® M1000 plate reader (Tecan Austria GmbH). The half-maximal inhibitory concentration (IC_{50}) values were determined using GraphPad Prism software.

2.5. Xenograft studies in mice

Animal studies were carried out in strict accordance with the recommendations of the Institutional Animal Care and Use Committee of the University of Texas at Houston (Protocol number AWC-19-0085 and AWC-21-0094). For SKNAS and SKNBD2 xenograft studies, female 9-10-week-old nu/nu mice (Charles River Laboratories) were subcutaneously inoculated with 5×10^6 cells in 1:1 mixture with Matrigel (BD Biosciences). After 2 weeks, when tumor size reached approximately ~100 mm^3, mice were randomized and given vehicle (PBS), R291-SG3199 or R299-SG3199 at the indicated dose levels and dosing frequency by intraperitoneal injection. Mice were routinely monitored for morbidity and mortality. Tumor volumes were measured bi-weekly and estimated by the formula: tumor volume = $(\text{length} \times \text{width}^2)/^2$.

2.6. Statistical analysis

All data were analyzed using GraphPad Prism software. Data are expressed as mean ± SEM or SD as indicated in the Results section. For tumor volume analysis, one-way ANOVA with Dunnett's multiple comparison test or Student's unpaired two-tailed t-test for two-group comparisons was employed. Survival data were analyzed using Kaplan-Meier analysis with Log-rank (Mantel-Cox) test for P value calculation. $P \leqslant 0.05$ was considered statistically significant.

3. Results and Discussion

An RSPO2 furin domain mutant that retains high affinity binding to LGR4/5 without potentiating Wnt/β-catenin signaling was identified. Of the four RSPOs, RSPO4 furin domain has the highest affinity to LGR4/5/6 with RSPO2 being a close second[41, 42]. RSPO2 is also unique for its high affinity binding to RNF43/ZNRF3 in the absence of LGR4/5/6[41, 43]. We then evaluated the potential use of RSPO2 furin domain peptibody for drug conjugation. X-ray crystal structure data showed that M68 and Q70 of RSPO2 furin-1 domain are critical to binding to RNF43/ZNRF3 and thus essential for potentiating of Wnt/β-catenin signaling[43, 44]

(Fig. 1A). Previously, we fused wild-type RSPO2 furin domain to human IgG1-Fc domain to create a peptibody designated R203 (Fig. 1A). We first generated a Q70R mutant called R206, similar to that of RSPO4 (Fig.1). Unlike RSPO4, mutation of Q70R alone was only able to partially inactivate W/β-catenin signaling[43] (Fig. 1D). We then evaluated various mutations of M68 in combination with Q70R and found that the M68T/Q70R combination (designated R232, Fig. 1A) led to a near total loss of activity in potentiating Wnt/β-catenin signaling (Fig. 1C-D). In binding analysis, R232 showed high affinity binding to cells expressing either LGR4 (Kd = 0.2 nM) or LGR5 (Kd = 0.3 nM) (Fig. 1E), similar to that of wild-type RSPO2 peptibody R203[41], with little binding to vector control cells (Fig. 1C-D).

For the conjugation of linker-payload, we introduced an N297A change into the glycosylation site of the Fc domain to create the peptide designated R291 that has a glutamine acceptor site (Q295) for the microbial transglutaminase[45] (Fig. 1A). For a control peptibody, we generated R299 which has two mutations in RSPO2 furin-2 domain (F105A/F109A) that abolishes binding to LGR4/5/6 based on crystal structure data of RSPO2 binding to LGR5 [44] (Fig. 1A). Binding analysis confirmed that R291 had high affinity binding to LGR5 (Kd = 0. 34 nM) whereas R299 has much reduced binding (Fig. 1D). To evaluate the potential of RSPO2 furin domain peptibodies for drug delivery, we conjugated the potent, PBD-based cytotoxin SG3199 to R291 and R299 using a chemoenzymatic method [33, 45, 46](Fig. 2A). A PEG4-azide was first attached to R291/R299 with microbial transglutaminase and complete conjugation was confirmed by mass spectrometry. DBCO-PEG8-VA-PAB-SG3199 was then linked to the azide through click chemistry and the resulting PDCs (R291-SG3199 and R299-SG3199) showed complete conjugation, which were confirmed to have two payloads per peptibody using mass spectrometry (Fig. 2B-C). Binding analysis showed that R291-SG3199, similar to unconjugated R291, retained high affinity binding to cells expressing LGR4, LGR5, or LGR6 whereas R299-SG3199 had much lower affinity binding (Fig. 2D-I).

RSPO2 furin mutant peptibody conjugated with PBD had potent and specific cytotoxic activity against cancer cells expressing LGR4/5/6 in vitro. R291-SG3199 and R299-SG3199 were tested side-by-side in a panel of NB cell lines that express LGR5 at high levels as we showed previously [13, 33]. In CHP212 cells, R291-SG3199 showed an IC50 of 0.09 nM whereas the control PDC R299-SG3199 showed an IC50 of 4.9 nM (Fig. 3A). In CHP212-LGR5KO cells in which LGR5 was knocked out by CRISPR-Cas9 [33], both R291-SG3199 and R299-SG3199 displayed similar potency with an IC50 of approximately 10 nM (Fig. 3A). In two other NB cells expressing LGR5 (SKNBE2 and SKNAS) [31, 33], R291-SG3199 also showed

potent cytotoxic activity (IC50 = 0.01 nM) whereas R299-SG3199 was much less potent (Fig. 3B). These results indicate that R291-SG3199 has potent and specific cytotoxic activity in NB cells expressing LGR5.

We then tested the two PDCs in a panel of colorectal cancer cells expressing LGR4, LGR5 and/ or LGR6 both as we described in a preprint [47]. In HT29 cells which express only LGR4, R291-SG3199 has IC50 of 0.1 nM while R299-SG3199 has IC50 of 5 nM (Fig. 4A). In LoVo and SW620 cells which express all three receptors at various levels[39], R291-SG3199 had IC50 of ~0.01 nM whereas R299-SG3199 displayed IC50 of ~1 nM (Fig. 4B-C). In RKO cells which express none of the three LGRs based CCLE's RNA-seq data, R291-SG3199 and R299-SG3199 showed no cytotoxic activity (Fig. 4D). Overall, these results show that R291-SG3199 has potent and specific cytotoxic activity against cancer cell lines expressing any of LGR4/5/6 or their combination. The cytotoxic activity of the control PDC R299-SG3199, though being much less potent than R291-SG3199, is most likely due to non-specific uptake by the cancer cells such as pinocytosis or residual binding activity to LGR4/5/6.

R291-SG3199 had robust anti-tumor activity in NB xenograft models in vivo. To evaluate the activity of RSPO2-based PDC in vivo, we tested R291-SG3199 in xenograft models of NB cell lines SKNAS and SKNBE2. For the SKNAS model, R291-SG3199 was given at 0.15 mg/kg and 0.3 mg/kg, twice per week, along with vehicle control, for 4 weeks. As Shown in Fig. 4A, R291-SG3199 showed reduction in tumor growth, with the low dose (0.15 mg/kg) reducing tumor growth by 45% ($p = 0.12$ vs vehicle, One-Way ANOVA) and the high dose (0.3 mg/kg) reducing tumor growth by 87% ($p = 0.002$ vs vehicle). Importantly, both R291-SG3199 groups extended survival significantly, with median survival of 39 days for the low dose group vs 25 days for the vehicle group ($p = 0.001$, log-rank test), and 46 days for the high dose group ($p < 0.0001$ vs vehicle, log-rank test). No major adverse effect was observed with no significant difference found in body weights among the groups, suggesting that the PDC was tolerated at these dose levels. We then evaluated R291-SG3199 in xenograft models of the NB cell line SKNBE2. The PDC was given at 0.3 mg/kg, twice per week for a total of eight doses. As shown in Fig. 4C, R291-SG3199 showed significant inhibition of tumor growth, with a 73% reduction ($p = 0.03$ vs vehicle control, T-test) in tumor growth as measured on Day 25 (the last day before the vehicle group has animals sacrificed). The PDC also extended survival significantly, with median survival of 61 days vs 25 days for the vehicle control group ($p < 0.0001$, log rank-test). These in vivo results demonstrated that R291-SG3199 was able to

significantly inhibit tumor growth at 0.3 mg/kg, which is approximately twice the human dose level of the SG3199-based ADC loncastuximab tesirine [46].

RSPO2 furin mutant peptibody conjugated with CPT2 had potent and specific cytotoxic activity against cancer cells expressing LGR4/5 in vitro and in vivo. Given the lack of total inhibition of tumor growth by R291-SG3199 in NB xenograft models in vivo and the limitation of dosing levels of PBD-based ADCs due to the extremely high potency of PBDs [46], we reasoned that conjugation of RSPO2-based peptibodies with CPT2 may enhance efficacy without increasing toxicity. Previously, we generated a PDC (R462-CPT2) using an RSPO4-based peptibody called R462 with close to 8 drugs per peptibody [39]. Toward this purpose, we replaced the N295A change of R291 and R299 with N295Q and created R290 and R296, respectively (Fig. 5A). Introduction of N295Q created two Gln residues in each Fc domain that can be conjugated with a bis-Azide linker to enable the conjugation of 8 drugs per peptibody [39, 48]. R290 showed high affinity binding to LGR5, just like R291, whereas R296 had little affinity (Fig. 5D-F). R290 and R296 were then conjugated with bis-azide linker first using microbial transglutaminase, followed by linking to DBCO-PEG8-PKG-CPT2 as described for R462 and R465 [39]. The resulting PDCs, R290-CPT2 and R296-CPT2, were confirmed to have ~8 molecules per peptibody by mass spectrometry (Fig. 5C). R290-CPT2 and R296-CPT2 were then tested in binding to HEK293T cells expressing LGR4, LGR5, or LGR6. Similar to the unconjugated R290 and R296, R290-CPT2 retained high affinity binding to all three receptors whereas R296-CPT2 showed low binding with reduced affinity (Fig. 5G-I). We then tested cytotoxic activity of R290-CPT2 and R296-CPT2 in cancer cell lines side-by-side. As shown in Fig. 6, R290-CPT2 showed IC50 of 0.9 nM, 0.3 nM, and 0.5 nM in SKNAS, SKNBE, and LOVO cells, respectively whereas R296-CPT2 had IC50 of 24, 20, and 21 nM, respectively. These results suggest that R290-CPT2 had potent and specific cytotoxic activity**.** Next, we tested R290-CPT2 in xenograft model of SKNAS cell in vivo. R290-CPT2 was given at 5.0 mg/kg, twice per week, similar to that of R291-SG3199, for a total of 6 doses. As shown in Fig. 6D, R290-CPT2 inhibited tumor growth by 77% ($p = 0.005$ vs vehicle on Day 14) and extended survival significantly (median survival of 37 days vs 19 days for vehicle, $p = 0.0001$, log-rank test). Overall, these results demonstrated that RSPO2 peptibody conjugated CPT2 had potent anti-tumor activity in vitro and in vivo.

LGR4/5/6 are often co-expressed or alternately expressed at moderate to high levels in gastrointestinal cancers. In NB, LGR5 is highly expressed in high-risk tumors whereas LGR4 is expressed at moderate levels [33]. Simultaneous targeting all three receptors of LGR4/5/6 may

offer increased efficacy and overcome tumor cell plasticity due to inter-conversion of LGR5-positive and -negative cells[22, 26], we set out to develop a strategy that utilizes a mutant ligand of LGR4/5/6 that retains high affinity receptor binding without potentiating Wnt/β-catenin signaling[38]. Here we generated new peptibodies based on mutant form of RSPO2 furin domain and conjugated with either PBD or CPT-derived payloads [49]. CPT-derived payloads are now the leading class for ADC development due to its success in solid tumors, and irinotecan, a CPT derivative, is an effective chemotherapy against CRC and NB.

RSPO2 and RSPO4 are approximate 50% identical in the furin domain, yet RSPO2 is much more potent than RSPO4 in potentiating Wnt/β-catenin signaling as RSPO2 is able to inhibit RNF43/ZNRF3 in the absence of LGR4/5/6 [41, 50]. We explored the use of RSPO2 furin domain for drug conjugation based on the potential for longer in vivo stability following fusion of IgG1-Fc and high affinity for LGR4 [42]. Mutation of two residues (M68T and Q70R) are required to abolish its activity in potentiating Wnt/β-catenin signaling (Fig. 1D), consistent with data from others[44]. The double mutation had no effect on binding affinity to LGR4/5/6, making it a potential candidate for conjugation.

When conjugated with two molecules of the PBD analog SG3199, R291-SG3199 had good solubility and showed high potency in cell lines expressing any of LGR4/5/6. This potency is higher than that of an anti-LGR5 antibody (called 8F2) conjugated with the same linker-payload[33], suggesting that natural ligand-based drug conjugate may target LGR5 more effectively. However, 8F2-SG3199 and R291-SG3199 showed similar efficacy in vivo despite the much higher cytotoxic potency of R291-SG3199 in vitro. The most likely explanation is that the half-life of R291-SG3199 is predicted to be much shorter than 8F2-SG3199 in vivo. When conjugated with eight molecules of CPT2, R290-CPT2 showed cytotoxic potencies similar to those of the RSPO4 furin-domain-based PDC R462-CPT2 across the CRC cell lines [39], suggesting that RSPO2 and RSPO4 furin domain induced internalization of LGR4//5/6 with similar potency and efficacy.

In conclusion, we generated two new peptibodies based on a mutant RSPO2 furin domain that showed high affinity, specific binding to LGR4/5/6 without potentiating Wnt/β-catenin signaling, and their drug conjugate displayed potent cytotoxic activity in CRC and NB cell lines expressing any of LGR4/5/6 in vitro, and robust anti-tumor efficacy in vivo without major adverse effect. Future studies will focus on optimizing the in vivo stability of the peptibody.

Acknowledgements

This work was supported in part by funding from the Cancer Prevention and Research Institute of Texas (CPRIT) RP220169 (to Q.J.L.) and RP210119 (to Q.J.L.), from the National Cancer Institute of the National Institutes of Health under grant numbers R21CA267381 (to Q.J.L.) and R41CA281553 (to J.C. and Q.J.L), and the Janice David Gordon for Bowel Cancer Research Endowment (to Q.J.L.).

References

1. McDonald, T., et al., *Identification and cloning of an orphan G protein-coupled receptor of the glycoprotein hormone receptor subfamily.* Biochem Biophys Res Commun, 1998. **247**(2): p. 266-70.
2. Hsu, S.Y., S.G. Liang, and A.J. Hsueh, *Characterization of two LGR genes homologous to gonadotropin and thyrotropin receptors with extracellular leucine-rich repeats and a G protein-coupled, seven-transmembrane region.* Mol Endocrinol, 1998. **12**(12): p. 1830-45.
3. Loh, E.D., et al., *Chromosomal localization of GPR48, a novel glycoprotein hormone receptor like GPCR, in human and mouse with radiation hybrid and interspecific backcross mapping.* Cytogenet Cell Genet, 2000. **89**(1-2): p. 2-5.
4. Sato, T., et al., *Single Lgr5 stem cells build crypt-villus structures in vitro without a mesenchymal niche.* Nature, 2009. **459**(7244): p. 262-5.
5. Barker, N. and H. Clevers, *Leucine-rich repeat-containing G-protein-coupled receptors as markers of adult stem cells.* Gastroenterology, 2010. **138**(5): p. 1681-96.
6. de Lau, W.B., B. Snel, and H.C. Clevers, *The R-spondin protein family.* Genome Biol, 2012. **13**(3): p. 242.
7. Carmon, K.S., et al., *R-spondins function as ligands of the orphan receptors LGR4 and LGR5 to regulate Wnt/beta-catenin signaling.* Proc Natl Acad Sci U S A, 2011. **108**(28): p. 11452-7.
8. de Lau, W., et al., *Lgr5 homologues associate with Wnt receptors and mediate R-spondin signalling.* Nature, 2011. **476**(7360): p. 293-7.
9. Glinka, A., et al., *LGR4 and LGR5 are R-spondin receptors mediating Wnt/beta-catenin and Wnt/PCP signalling.* EMBO Rep, 2011. **12**(10): p. 1055-61.
10. Gong, X., et al., *LGR6 Is a High Affinity Receptor of R-Spondins and Potentially Functions as a Tumor Suppressor.* PLoS One, 2012. **7**(5): p. e37137.
11. Hao, H.X., et al., *ZNRF3 promotes Wnt receptor turnover in an R-spondin-sensitive manner.* Nature, 2012. **485**(7397): p. 195-200.
12. Koo, B.K., et al., *Tumour suppressor RNF43 is a stem-cell E3 ligase that induces endocytosis of Wnt receptors.* Nature, 2012. **488**(7413): p. 665-9.
13. Park, S., et al., *Unlike LGR4, LGR5 potentiates Wnt-beta-catenin signaling without sequestering E3 ligases.* Sci Signal, 2020. **13**(660).
14. Wang, L., et al., *Structural insights into the LGR4-RSPO2-ZNRF3 complexes regulating WNT/beta-catenin signaling.* Nat Commun, 2025. **16**(1): p. 362.
15. Gao, Y., et al., *Up-regulation of GPR48 induced by down-regulation of p27Kip1 enhances carcinoma cell invasiveness and metastasis.* Cancer Res, 2006. **66**(24): p. 11623-31.
16. Yi, J., et al., *Analysis of LGR4 Receptor Distribution in Human and Mouse Tissues.* PLoS One, 2013. **8**(10): p. e78144.
17. Gugger, M., et al., *GPR87 is an overexpressed G-protein coupled receptor in squamous cell carcinoma of the lung.* Dis Markers, 2008. **24**(1): p. 41-50.

18. Gong, X., et al., *Aberrant RSPO3-LGR4 signaling in Keap1-deficient lung adenocarcinomas promotes tumor aggressiveness.* Oncogene, 2015. **34**(36): p. 4692-701.
19. Yue, Z., et al., *LGR4 modulates breast cancer initiation, metastasis, and cancer stem cells.* FASEB J, 2018. **32**(5): p. 2422-2437.
20. Junttila, M.R., et al., *Targeting LGR5+ cells with an antibody-drug conjugate for the treatment of colon cancer.* Sci Transl Med, 2015. **7**(314): p. 314ra186.
21. Vermeulen, L., et al., *Single-cell cloning of colon cancer stem cells reveals a multi-lineage differentiation capacity.* Proc Natl Acad Sci U S A, 2008. **105**(36): p. 13427-32.
22. Kobayashi, S., et al., *LGR5-positive colon cancer stem cells interconvert with drug-resistant LGR5-negative cells and are capable of tumor reconstitution.* Stem Cells, 2012. **30**(12): p. 2631-44.
23. Kemper, K., et al., *Monoclonal antibodies against Lgr5 identify human colorectal cancer stem cells.* Stem Cells, 2012. **30**(11): p. 2378-86.
24. Huang, P.Y., et al., *Lgr6 is a stem cell marker in mouse skin squamous cell carcinoma.* Nat Genet, 2017. **49**(11): p. 1624-1632.
25. Shimokawa, M., et al., *Visualization and targeting of LGR5(+) human colon cancer stem cells.* Nature, 2017. **545**(7653): p. 187-192.
26. de Sousa e Melo, F., et al., *A distinct role for Lgr5(+) stem cells in primary and metastatic colon cancer.* Nature, 2017. **543**(7647): p. 676-680.
27. Kim, S.K., et al., *A nineteen gene-based risk score classifier predicts prognosis of colorectal cancer patients.* Mol Oncol, 2014. **8**(8): p. 1653-66.
28. Leto, S.M., et al., *XENTURION, a multidimensional resource of xenografts and tumoroids from metastatic colorectal cancer patients for population-level translational oncology.* bioRxiv, 2023: p. 2023.07.10.548375.
29. Coulon, A., et al., *Functional sphere profiling reveals the complexity of neuroblastoma tumor-initiating cell model.* Neoplasia, 2011. **13**(10): p. 991-1004.
30. Forgham, H., et al., *Stem Cell Markers in Neuroblastoma-An Emerging Role for LGR5.* Front Cell Dev Biol, 2015. **3**: p. 77.
31. Vieira, G.C., et al., *LGR5 regulates pro-survival MEK/ERK and proliferative Wnt/beta-catenin signalling in neuroblastoma.* Oncotarget, 2015. **6**(37): p. 40053-67.
32. Giwa, A., et al., *Identification of novel prognostic markers of survival time in high-risk neuroblastoma using gene expression profiles.* Oncotarget, 2020. **11**(46): p. 4293-4305.
33. Tu, J., et al., *Antitumor Activity of a Pyrrolobenzodiazepine Antibody-Drug Conjugate Targeting LGR5 in Preclinical Models of Neuroblastoma.* Pharmaceutics, 2024. **16**(7).
34. Balamuth, N.J., et al., *Serial transcriptome analysis and cross-species integration identifies centromere-associated protein E as a novel neuroblastoma target.* Cancer Res, 2010. **70**(7): p. 2749-58.
35. Clark-Corrigall, J., et al., *Elevated Expression of LGR5 and WNT Signaling Factors in Neuroblastoma Cells With Acquired Drug Resistance.* Cancer Invest, 2023. **41**(2): p. 173-182.
36. Carter, P.J. and P.D. Senter, *Antibody-drug conjugates for cancer therapy.* Cancer J, 2008. **14**(3): p. 154-69.
37. Dumontet, C., et al., *Antibody-drug conjugates come of age in oncology.* Nat Rev Drug Discov, 2023. **22**(8): p. 641-661.
38. Cui, J., et al., *Drug Conjugates of Antagonistic R-Spondin 4 Mutant for Simultaneous Targeting of Leucine-Rich Repeat-Containing G Protein-Coupled Receptors 4/5/6 for Cancer Treatment.* J Med Chem, 2021. **64**(17): p. 12572-12581.
39. Toh, Y., et al., *Anti-tumor activity of camptothecin analog conjugate of a RSPO4-based peptibody targeting LGR4/5/6 in preclinical models of colorectal cancer.* bioRxiv, 2024.

40. Shalem, O., et al., *Genome-scale CRISPR-Cas9 knockout screening in human cells.* Science, 2014. **343**(6166): p. 84-7.
41. Park, S., et al., *Differential activities and mechanisms of the four R-spondins in potentiating Wnt/beta-catenin signaling.* J Biol Chem, 2018. **293**(25): p. 9759-9769.
42. Warner, M.L., T. Bell, and A.A. Pioszak, *Engineering high-potency R-spondin adult stem cell growth factors.* Mol Pharmacol, 2015. **87**(3): p. 410-20.
43. Zebisch, M., et al., *Structural and molecular basis of ZNRF3/RNF43 transmembrane ubiquitin ligase inhibition by the Wnt agonist R-spondin.* Nat Commun, 2013. **4**: p. 2787.
44. Zebisch, M. and E.Y. Jones, *Crystal structure of R-spondin 2 in complex with the ectodomains of its receptors LGR5 and ZNRF3.* J Struct Biol, 2015. **191**(2): p. 149-55.
45. Lhospice, F., et al., *Site-Specific Conjugation of Monomethyl Auristatin E to Anti-CD30 Antibodies Improves Their Pharmacokinetics and Therapeutic Index in Rodent Models.* Mol Pharm, 2015. **12**(6): p. 1863-71.
46. Zammarchi, F., et al., *ADCT-402, a PBD dimer-containing antibody drug conjugate targeting CD19-expressing malignancies.* Blood, 2018. **131**(10): p. 1094-1105.
47. Yukimatsu Toh, L.W., Jianghua Tu, Zhengdong Liang, Adela Aldana, Li Li, , S.P. Jake J. Wen, Rowe H. Julie, Martha E. Hensel, Carolyn L. Hodo, , and K.S.C. Rick A. Finch, and Qingyun J. Liu, *Anti-tumor activity of camptothecin analog conjugate of a RSPO4-based peptibody targeting LGR4/5/6 in preclinical models of colorectal cancer. .* BioRXiv(Preprint), 2024.
48. Anami, Y., et al., *Enzymatic conjugation using branched linkers for constructing homogeneous antibody-drug conjugates with high potency.* Org Biomol Chem, 2017. **15**(26): p. 5635-5642.
49. Lyski, R.D., et al., *Development of Novel Antibody-Camptothecin Conjugates.* Mol Cancer Ther, 2021. **20**(2): p. 329-339.
50. Lebensohn, A.M. and R. Rohatgi, *R-spondins can potentiate WNT signaling without LGRs.* Elife, 2018. **7**.

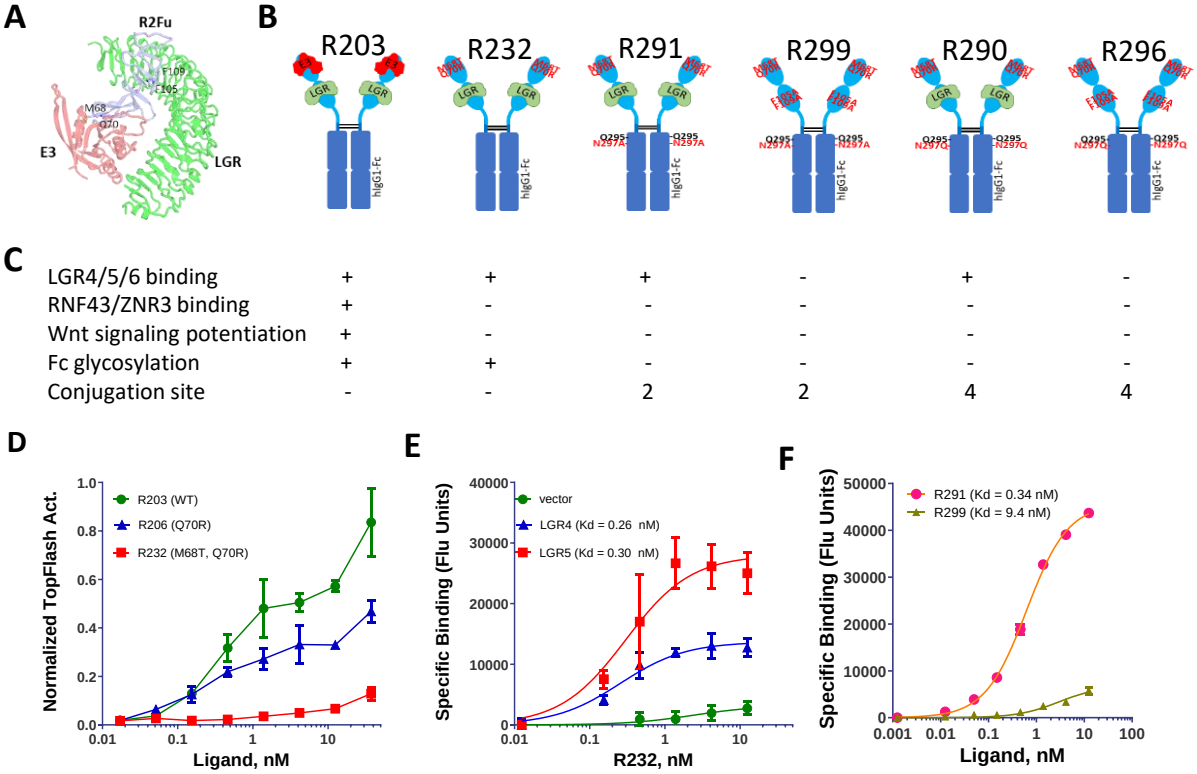

Figure 1. Generation of RSPO2-furin Fc fusion protein and characterization of their binding affinities. A, Structure model of RSPO2 furin domain bound to E3 ligase and LGR4ECD. B, Schematic diagram of RSPO2 furin domain-based peptibodies with various mutations. C, Summary of binding and signaling activity of the various RSPO2 furin peptibodies. D, Potentiation of Wnt/b-catenin signaling by R203, R206, and R232 in the TopFlash assay. E, Whole-cell binding of R232 to HEK293T cells stably expressing LGR4, LGR5 or vector control. F, Whole-cell binding of R291 and R299 to HEK293T cells stably expressing LGR5. Error bars are SEM (N = 2-3).

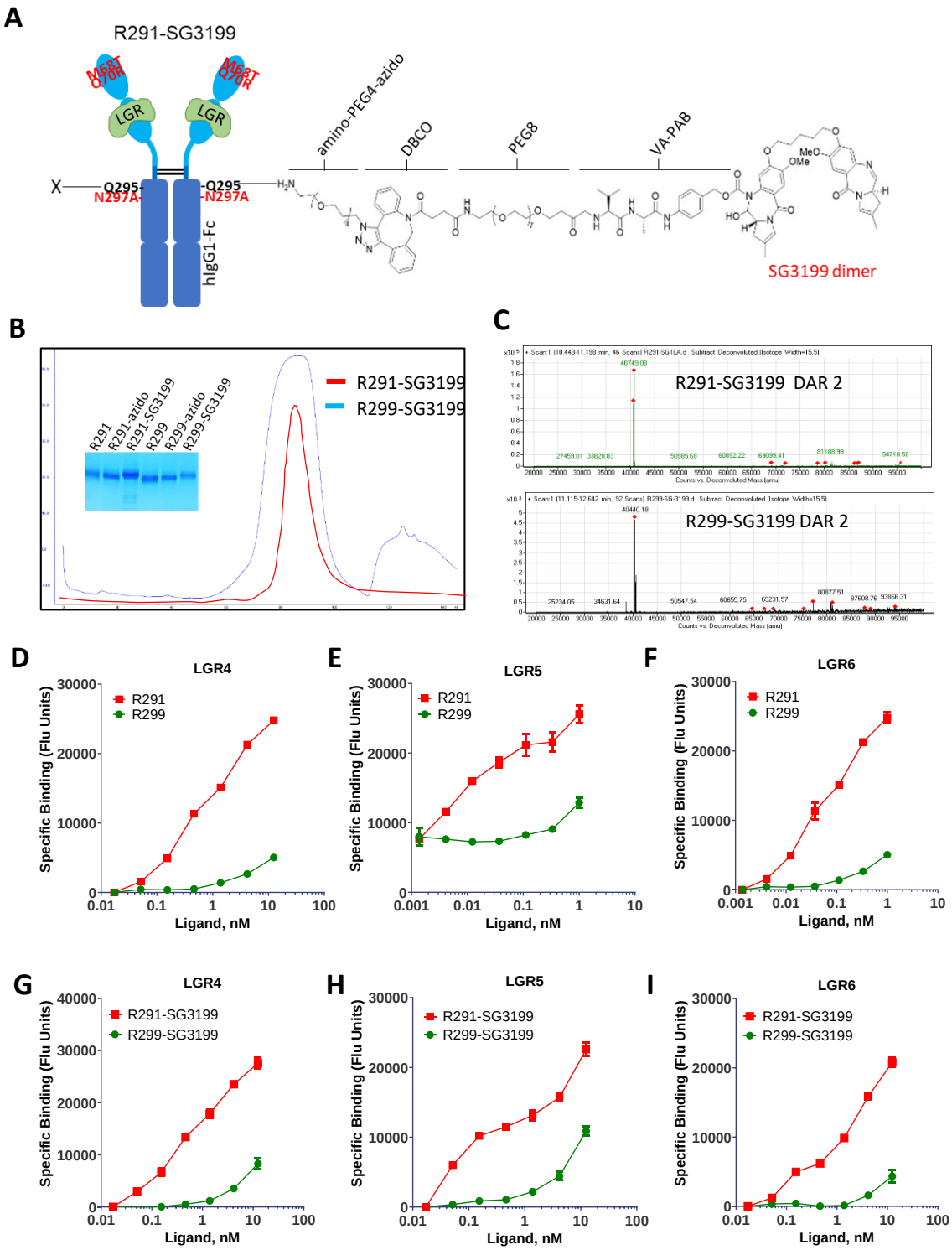

Figure 2. R291 and R299 PDC synthesis and conjugation. A, Schematic diagram of R291/R299 conjugated with SG3199. B, Chromatogram of R291- and R299-SG3199 in gel filtration and Coomassie staining of SDS-PAGE of R291/R299 before and after conjugation. C, Mass spectrum of R291-SG3199 (top) and R299-SG3199 (bottom). D-F, Whole-cell binding of unconjugated R291 and R299 to HEK293T cells expressing LGR4 (D), LGR5 (E), and LGR6 (F). G-H, Whole-cell binding of R291-SG3199 and R299-SG3199 to HEK293T cells expressing LGR4 (G), LGR5 (H), and LGR6 (I). Error bars are SEM (N = 2-3).

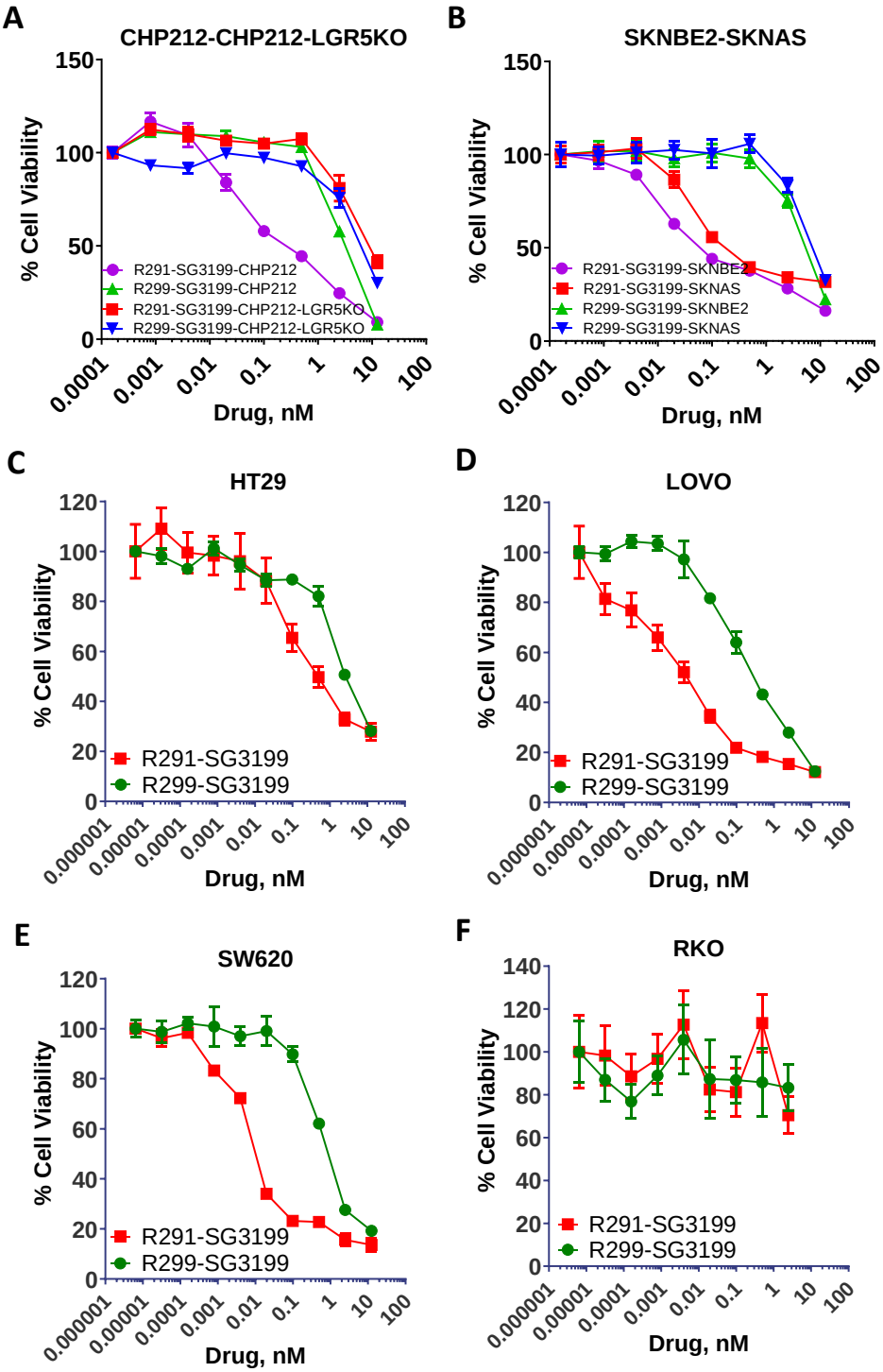

Figure 3. Cytotoxic activity of R291-SG3199 and R299-SG3199 in NB and CRC cell lines. A-B, NB cell lines CHP212 and CHP212-LGR5KO (A) and SKNBE2 and SKNAS (B). C-F, CRC cell lines HT29 (C), LOVO (D), SW620 (E), and RKO (F). Error bars are SEM (N = 2-3).

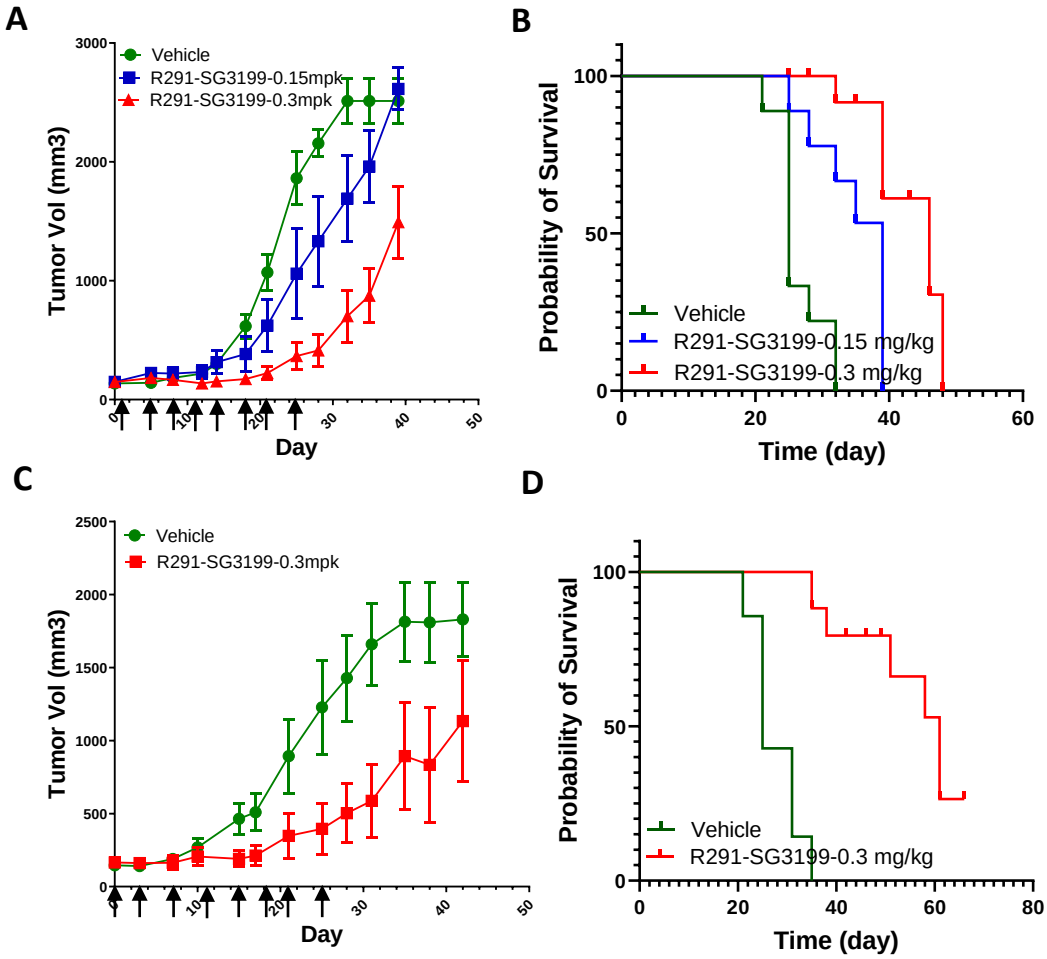

Figure 4. Anti-tumor activity of R291-SG3199 in xenograft models of NB cell lines. A, Tumor growth curves of SKNAS xenografts treated with vehicle (N = 9) or R291-SG3199 at 0.15 mg/kg (N = 8), or 0.3 mg/kg (N = 8). Injection days are marked by arrows. B, Kaplan-Meier survival plot of the study in A. C, Tumor growth curves of SKNBE2 xenografts treated with vehicle (N = 7) or R291-SG3199 at 0.3 mg/kg (N =8). Drug injection days are marked by arrows. D, Kaplan-Meier survival plot of the study in C.

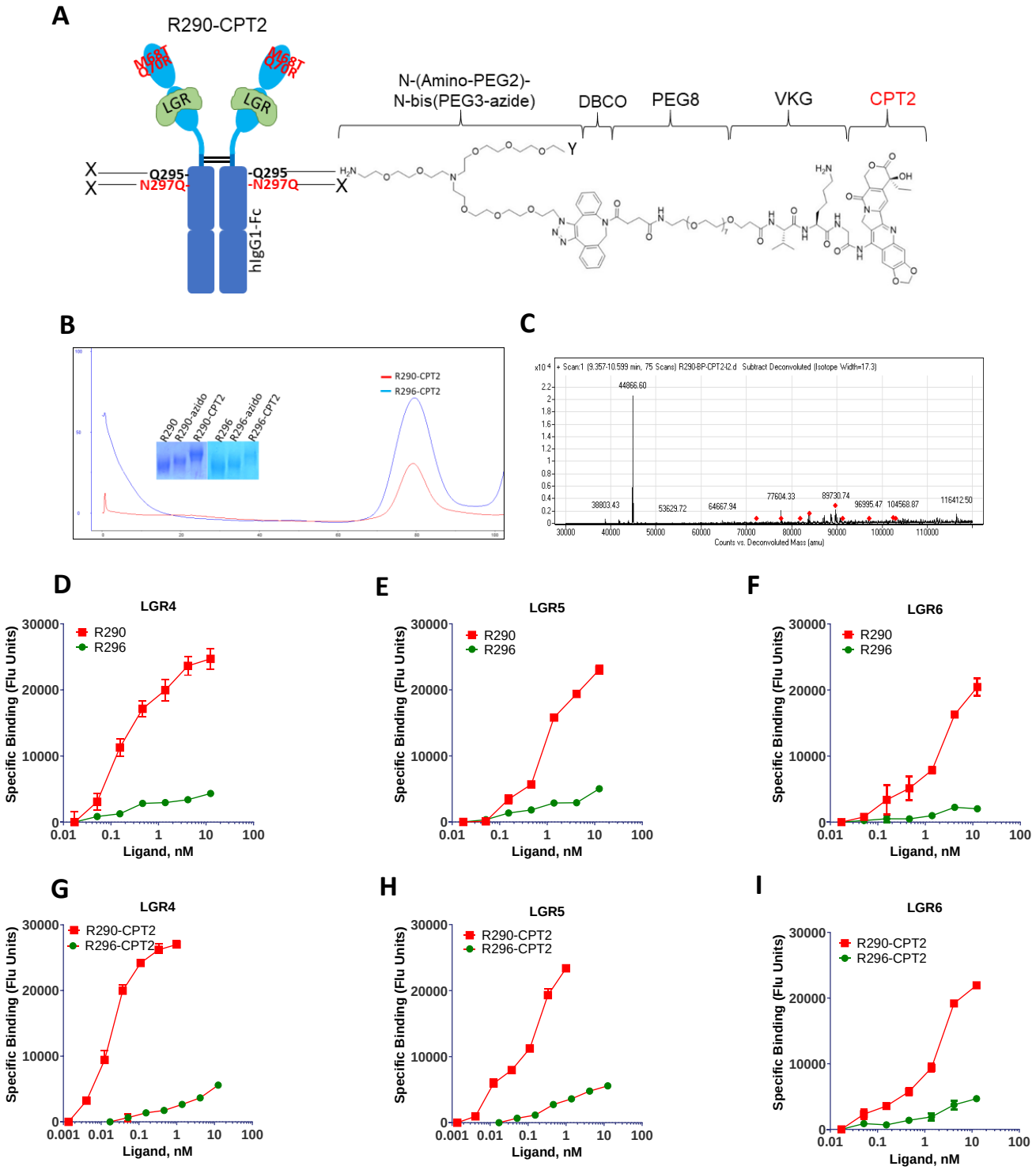

Figure 5. R290 and R296 PDC synthesis and conjugation. A, Schematic diagram of R290/R296 conjugated with CPT2. B, Chromatogram of R290- and R296-CPT2 in gel filtration and Coomassie staining of SDS-PAGE of R291/R299 before and after conjugation. C, Mass spectrum of R290-CPT2. D-F, Whole-cell binding of unconjugated R290 and R296 to HEK293T cells expressing LGR4 (D), LGR5 (E), and LGR6 (F). G-H, Whole-cell binding of R290-CPT2 and R296-CPT2 to HEK293T cells expressing LGR4 (G), LGR5 (H), and LGR6 (I). Error bars are SEM (N = 2-3).

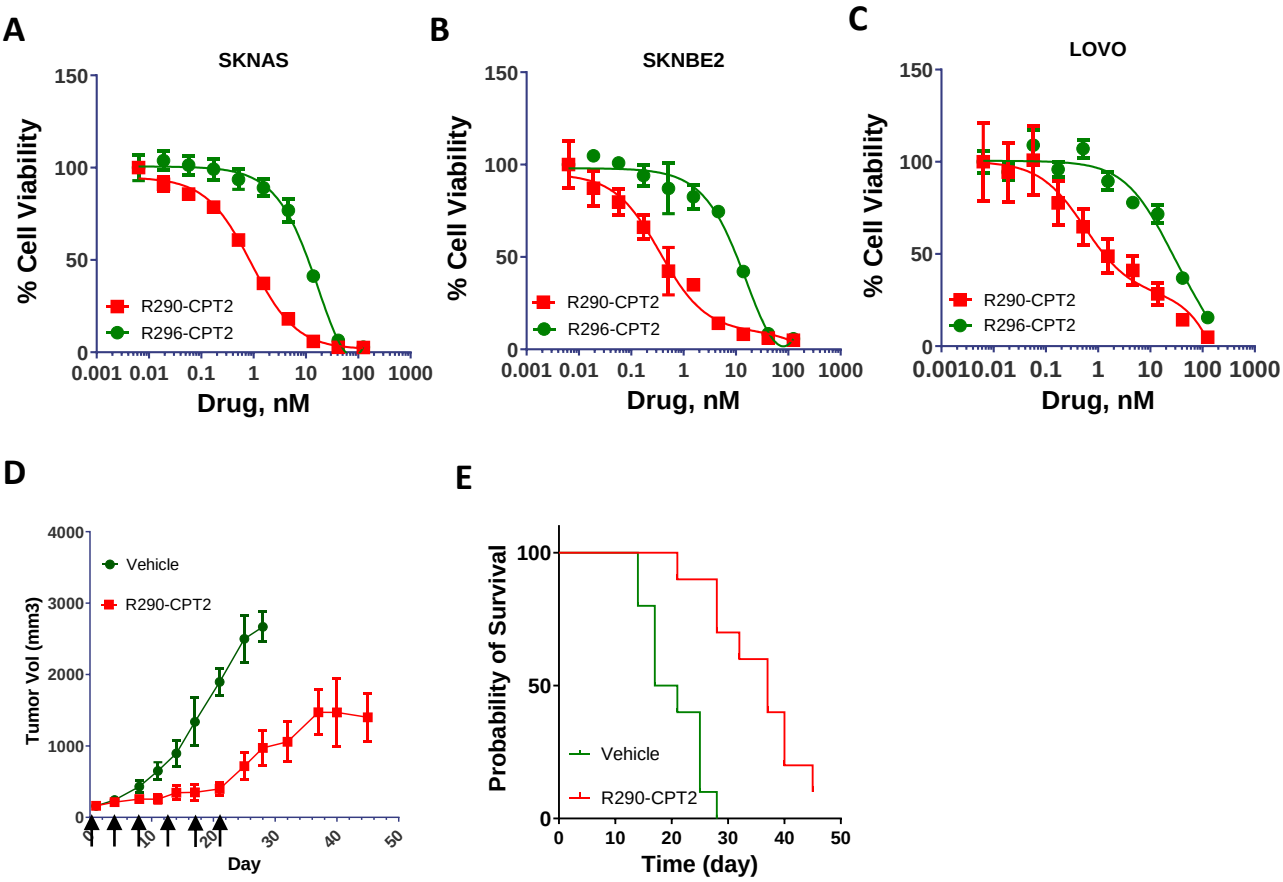

Figure 6. Activity of R290-CPT2 and R296-CPT2 in vitro and in vivo. A-C, Cytotoxic activity of R290-CPT2 and R296-CPT2 in SKNAS (A) and SKNBE2 (B), and LOVO cells (C). D, Tumor growth curves of SKNAS xenografts treated with vehicle or R290-CPT2 at 5 mg/kg (N = 10 per group). Injection days are marked by arrows. E, Kaplan-Meier survival plot of the study in D.